Toxicology 325 (2014) 1–11

Contents lists available at ScienceDirect

Toxicology

journal homepage: www.elsevier.com/locate/toxicol

Dose-dependent clearance kinetics of intratracheally administered titanium dioxide nanoparticles in rat lung

Naohide Shinohara [a,*], Yutaka Oshima [b], Toshio Kobayashi [b], Nobuya Imatanaka [c], Makoto Nakai [b], Takayuki Ichinose [d], Takeshi Sasaki [e], Guihua Zhang [a], Hiroko Fukui [a], Masashi Gamo [a]

[a] National Institute of Advanced Industrial Science and Technology (AIST), Tsukuba, Ibaraki 305-8569, Japan
[b] Chemicals Evaluation and Research Institute (CERI), Hita, Oita 877-0061, Japan
[c] Chemicals Evaluation and Research Institute (CERI), Bunkyo, Tokyo 112-0004, Japan
[d] Toray Research Center, Inc., Otsu, Shiga 520-8567, Japan
[e] National Institute of Advanced Industrial Science and Technology (AIST), Tsukuba, Ibaraki 305-8565, Japan

ARTICLE INFO

Article history:
Received 17 June 2014
Received in revised form 8 August 2014
Accepted 8 August 2014
Available online 13 August 2014

Keywords:
Nanomaterial
Overload
Distribution
Clearance
Toxicokinetics
Compartment model

ABSTRACT

AEROSIL® P25 titanium dioxide (TiO_2) nanoparticles dispersed in 0.2% disodium phosphate solution were intratracheally administered to male F344 rats at doses of 0 (control), 0.375, 0.75, 1.5, 3.0, and 6.0 mg/kg. The rats were sacrificed under anesthesia at 1 day, 3 days, 7 days, 4 weeks, 13 weeks, and 26 weeks after administration. Ti levels in various pulmonary and extrapulmonary organs were determined using sensitive inductively coupled plasma sector field mass spectrometry. One day after administration, the lungs contained 62–83% of TiO_2 administered dose. Twenty-six weeks after administration, the lungs retained 6.6–8.9% of the TiO_2 administered at the 0.375, 0.75, and 1.5 mg/kg doses, and 13% and 31% of the TiO_2 administered at the 3.0 and 6.0 mg/kg doses, respectively. The pulmonary clearance rate constants from compartment 1, k_1, were estimated using a 2-compartment model and were found to be higher for the 0.375 and 0.75 mg/kg doses of TiO_2 (0.030/day for both) than for TiO_2 doses of 1.5–6.0 mg/kg (0.014–0.022/day). The translocation rate constants from compartment 1 to 2, k_{12}, were estimated to be 0.015 and 0.018/day for the 0.375 and 0.75 mg/kg doses, and 0.0025–0.0092/day for doses of 1.5–6.0 mg/kg. The pulmonary clearance rate constants from compartment 2, k_2, were estimated to be 0.0086 and 0.0093/day for doses of 0.375 and 0.75 mg/kg, and 0–0.00082/day for 1.5–6.0 mg/kg doses. Translocation of TiO_2 from the lungs to the thoracic lymph nodes increased in a time- and dose-dependent manner, accounting for 0.10–3.4% of the administered dose at 26 weeks. The measured thoracic lymph node burdens were a much better fit to the thoracic lymph node burdens estimated assuming translocation from compartment 1 to the thoracic lymph nodes, rather than those estimated assuming translocation from compartment 2 to the thoracic lymph nodes. The translocation rate constants from the lungs to the thoracic lymph nodes, $k_{Lung \rightarrow Lym}$, were 0.000037–0.00081/day, and these also increased with increasing doses of TiO_2. Although a small amount of TiO_2 had translocated to the liver by 3 days after the administration (0.0023–0.012% of the highest dose administered, 6.0 mg/kg), translocation to the other extrapulmonary organs was not detected.

1. Introduction

The safety of nanomaterials has been the focus of worldwide concern because of the lack of information available regarding their potential risks for workers and the general population. Therefore, the toxicity of nanomaterials has been tested internationally. Nano-sized titanium dioxide (TiO_2) particles (primary particle size <100 nm), one of the most typical industrial nanomaterials, have been utilized in sunscreen, cosmetics, and photo catalysis since the 1980s. Global demand for TiO_2 nanomaterials was estimated at 2100–2500 tons per year in 2008 (Fuji Chimera Research Institute, Inc., 2009). Since TiO_2 is water-insoluble and inert, it is generally regarded as having low toxicity in humans and is even used as an additive in food products. However, nano-sized particles may be more toxic or show a more widespread organ distribution than micron-sized particles

* Corresponding author. Tel.: +81 29 861 8415; fax: +81 29 861 8030.
E-mail address: n-shinohara@aist.go.jp (N. Shinohara).

http://dx.doi.org/10.1016/j.tox.2014.08.003

(Donaldson et al., 2001, 2004; Oberdörster et al., 2005; De Jong et al., 2008).

In order to evaluate the toxicity of TiO_2 nanoparticles, toxicokinetic data are beneficial. Since it is well established that pulmonary clearance of particles is inhibited following the administration of higher doses, a phenomenon known as overload (Morrow, 1992), it is important to evaluate the dose-dependency of pulmonary clearance when considering inhalation toxicity. In addition, after inhalation or intratracheal administration of TiO_2 nanoparticles, Ti have been detected in the lungs and lung-associated lymph nodes, while Ti levels in other organs such as the liver, spleen, kidneys, and brain were below the detection limit (Bermudez et al., 2004; Ma-Hock et al., 2009; van Ravenzwaay et al., 2009; Oyabu et al., 2013; Sager et al., 2008).

One-compartment models have been often used for the evaluation of pulmonary clearance (Bermudez et al., 2004; Oyabu et al., 2013). First order clearance rate constants for highly persistent substances often decrease as the observation period increases. Therefore, first order clearance rate constants estimated by using a 1-compatment model over different observation periods cannot be compared with each other. In addition, a 1-compartment model does not fit the measured burden closely. A two-compartment model was reported to provide a better fit to the measured burden and can be applied to evaluate both faster and slower clearances (Shinohara et al., 2010). However, there are no studies evaluating the clearance of TiO_2 nanoparticles from the lung using a 2-compartment model.

The present study aimed to elucidate dose-dependent pulmonary clearance kinetics and dose-dependent translocation kinetics to extrapulmonary organs of TiO_2 nanoparticle. In this study, we administered TiO_2 nanoparticles intratracheally to rats at 5 doses and investigated their pulmonary clearance and translocation from the lung to extrapulmonary organs over 26 weeks. We determined the TiO_2 burden in the lungs after sampling of bronchoalveolar lavage fluid (BALF), BALF, and trachea, as well as the thoracic lymph nodes (right and left posterior mediastinal lymph nodes, parathymic lymph nodes), liver, spleen, and kidneys using a highly sensitive inductively coupled plasma sector field mass spectroscopy (ICP-SFMS; double-focusing ICP-MS). The pulmonary clearance rate constants estimated using a classical 2-compartment model were compared over a range of doses. AEROSIL® P25 TiO_2 nanoparticles, which have often been employed for toxicity testing of TiO_2 nanoparticles and have been shown to induce lung inflammation (Rehn et al., 2003; Sager et al., 2008; Warheit et al., 2007) were used in the present study.

2. Material and methods

2.1. Preparation of TiO_2 suspension

AEROSIL® P25 TiO_2 nanoparticles (Evonik Industries, Germany), consisting of approximately 80% anatase and 20% rutile forms of TiO_2, were used in the present study. These spherical 21 nm particles had a specific surface of $50 \pm 15\ m^2/g$, and >99.5% purity (Catalog value; Nippon Aerosil Co., Ltd.).

P25 TiO_2 nanoparticles (2 g) were sonicated in 50 mL of 0.2% disodium phosphate solution (DSP) (food additive grade, Wako Pure Chemical Industries, Ltd. , Japan) for 3 h in an ultrasonic bath (5510J-MT; Branson Ultrasonics Co., USA) and then centrifuged at $1000 \times g$ for 30 min at 20 °C (CF16RXII and T15A41; Hitachi Koki Co., Ltd. , Japan). Supernatant (30 mL) was collected as stock suspension. The concentration of the stock suspension was determined by weight (AUW220D; Shimadzu Co., Japan) after drying in a thermostatic chamber (ON-300S; Asone Co., Japan). Suspensions of 0.375, 0.75, 1.5, 3.0, and 6.0 mg/mL were prepared for administration by diluting the stock suspension with 0.2% DSP. The size distribution and ζ potential of the TiO_2 nanoparticles in the administered suspension were determined by dynamic light scattering (DLS) (Zetasizer nano-ZS; Malvern Instruments Ltd., UK). The specific surface area of TiO_2 nanoparticles in administered suspension was determined using the BET-method after washing with pure water and drying in a thermostatic chamber.

2.2. Experimental procedure

All animal were treated in accordance with the guideline for the animal experiment of our laboratory which referred to the guidelines of Ministry of the Environment, Japan, Ministry of Health, Labour and Welfare, Japan, Ministry of Agriculture, Forestry and Fisheries, Japan, Ministry of Education, Culture, Sports, Science and Technology, Japan. The present experiment was approved by the Animal Care and Use Committee, Chemicals Evaluation and Research Institute, Japan, and by the Institutional Animal Care and Use Committee, National Institute of Advanced Industrial Science and Technology.

Male F344/DuCrlCrlj rats were obtained from Charles River Laboratories Japan, Inc. (Kanagawa, Japan). The animals were 12 weeks old with mean body weight of 246 g (range, 215–273 g) at the start of the study. Rats were anesthetized by isoflurane inhalation and treated by intratracheal administration of five concentrations of TiO_2 nanoparticles (0.375, 0.75, 1.5, 3.0, and 6.0 mg/mL) and negative control (0.2% DSP) at 1 mL/kg body weight using MicroSprayer® Aerosolizer (Model IA-1B-R for Rat; Penn-Century, Inc., USA).

Five rats in each group were euthanized and dissected at 1 day, 3 days, 7 days, 4 weeks, 13 weeks, and 26 weeks after TiO_2 nanoparticle administration. The animals were euthanized by exsanguination from the abdominal aorta under intraperitoneal pentobarbital anesthesia (50 mg/kg body weight). Thereafter, the trachea was cannulated with a disposable feeding needle, which was then tied in place. The lungs were lavaged with 7 mL of physiological saline freely flowing from 30 cm above the rat and this fluid was collected in a tube placed 30 cm below the rat. This lavage was performed twice and >90% of the 14 mL of lavage fluid was recovered. After BALF sampling, the lungs, trachea, right and left posterior mediastinal lymph nodes, parathymic lymph nodes, liver, kidneys, and spleen of each animal were dissected, rinsed with saline, and weighed.

2.3. Analysis

The Ti contents in the lungs after BALF sampling, BALF, trachea, right and left posterior mediastinal lymph nodes, parathymic lymph nodes, and liver of every animal were analyzed. The Ti contents in the kidneys and spleen of the negative control and highest dose groups were analyzed. In addition, the Ti contents in the stock suspension, drinking water, and food were also analyzed.

The lungs after BALF sampling, kidneys, and spleen were homogenized with 2 mL of ultrapure water (Milli-Q Advantage A10 Ultrapure Water Purification System, Merck Millipore, USA), and the liver was homogenized with 10 mL of ultrapure water. An electric homogenizer (PT10-35 Kinematica AG and NS-50; Microtec Co. Ltd., Japan) was used and the resulting homogenates were stored at < -30 °C until analysis.

All samples were treated with acid prior to determination of Ti levels. Nitric acid (HNO_3; 68%, 0.5 mL) and hydrogen peroxide (H_2O_2; 35%, 0.2 mL) were added to 0.1 mL of BALF, HNO_3 (1 mL), and sulfuric acid (H_2SO_4; 98%, 0.2 mL) were added to 1 g of homogenized tissues, HNO_3 (0.5 mL) and H_2SO_4 (0.1 mL) were added to whole lymph node samples, HNO_3 (1 mL) and H_2O_2 (0.3 mL) were added to 0.02 g of animal feed, and H_2SO_4 (0.5 mL) and hydrofluoric acid (HF; 38%, 0.5 mL) were added to 20 μL and 100 μL for high and low concentrations of the administered TiO_2 suspension, respectively. Drinking water was diluted 10-fold with 10% HNO_3 solution,

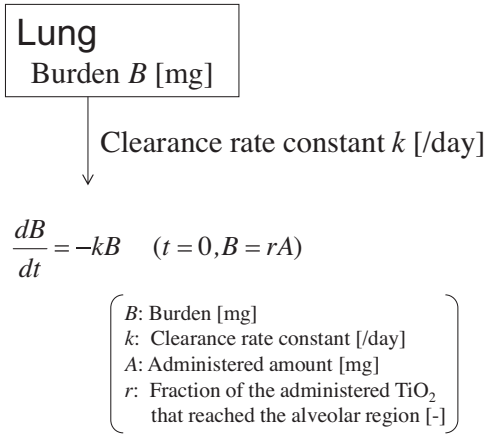

Fig. 1. 1-compartmental models for the clearance of TiO_2 nanoparticles. This model is expressed in a first-order decay equation with rate constant *k*.

with no subsequent handling. All acids used in the present study were ultrapure grade reagents (TAMAPURE-AA-100, Tama Chemicals Co., Ltd., Japan). The acidified samples (apart from drinking water) were placed in a 7 mL perfluoroalkylvinylether vessel, which was inserted into a 100 mL digestion vessel of a microwave sample preparation instrument (ETHOS 1; Milestone Srl Italy or Speedwave 4; Berghof, Germany), and they were heated to 180 °C for 20 min or 200 °C for 20 min. After cooling to 40 °C, the acid-treated samples, with the exception of the TiO_2 nanoparticle suspensions, were diluted to 5 mL (BALF and lymph nodes) or 10 mL (the other organs and feed) with ultrapure water (made by PURELAB Option-R 7 and PURELAB Flex UV from Veolia Water Solutions and Technologies, France). Samples of the acid-treated TiO_2 nanoparticle suspensions were heated on a hotplate for approximately 2 h until white fuming sulfuric acid was generated. After cooling, the solution was diluted to 50 mL with 10% HNO_3.

The sample Ti contents were then determined by ICP-SFMS using a Finnigan ELEMENT II (Thermo Fisher Scientific Inc., Germany), and the Ti content in the administered TiO_2 nanoparticle suspensions was determined by ICP atomic emission spectrometry (ICP-AES; SPS4000, SII NanoTechnology Inc., Japan). For ICP-SFMS, RF power was 1250 W, cool gas flow rate was 16 L/min, auxiliary gas flow rate was 0.87 L/min, sample gas flow rate was 0.870–0.965 L/min, additional gas flow rate was 0.080–0.180 L/min, mass resolution (*R*) was 4000, and the measured mass number m/z was 49. For ICP-AES, RF power was 1.3 kW, plasma gas flow rate was 16 L/min, additional gas flow rate was 0.5 L/min, carrier gas flow rate was 1.0 L/min, and wavelength was 334.941 nm. In the present study, ^{49}Ti (mass: 48.9479) was analyzed because its spectrum could be separated from the spectra of $^{33}S^{16}O$ (mass: 48.9666), $^{31}P^{18}O$ (mass: 48.9729), and $^{32}S^{16}O^{1}H$ (mass: 48.9748). Linearity of the calibration curves for ^{49}Ti using ICP-SFMS was good between 0 and 20 ng/mL of standard solution (0, 0.01, 0.05, 0.1, 1, 5, 10, and 20 ng/mL; $R^2 > 0.999$). Quality assurance data for the analysis were as previously described (Shinohara et al., 2014).

2.4. TiO_2 clearance analysis using decay model fitting

Both 1-compartment and 2-compartment models were employed in this study. The 1-compartment model assumed one clearance pathway from the lungs (Fig. 1). For the 2-compartment approach, two kinds of clearance pathway models were considered. Model A (Fig. 2A) assumed, direct clearance from the compartment 1, translocation from compartment 1 to 2, and clearance via compartment 2, while model B (Fig. 2B) assumed clearance from compartment 1 only, and reciprocal translocation between compartments 1 and 2.

The 1-compartment model can be represented by a 1-step clearance rate constant, as shown in Eq. (1), where *B* was the TiO_2 lung burden; *A* was the amount of TiO_2 administered (mg); *t* was the time elapsed after administration (day); *r* was the fraction of the administered TiO_2 that reached the alveolar region; and *k* was the clearance rate constant for the clearance (/day).

$$\frac{dB}{dt} = -kB \quad (t = 0,\ B = rA) \tag{1}$$

The 2-compartment model A can be represented by a 2-step clearance as shown in Eqs. (2) and (3), where B_1 was the TiO_2 burden

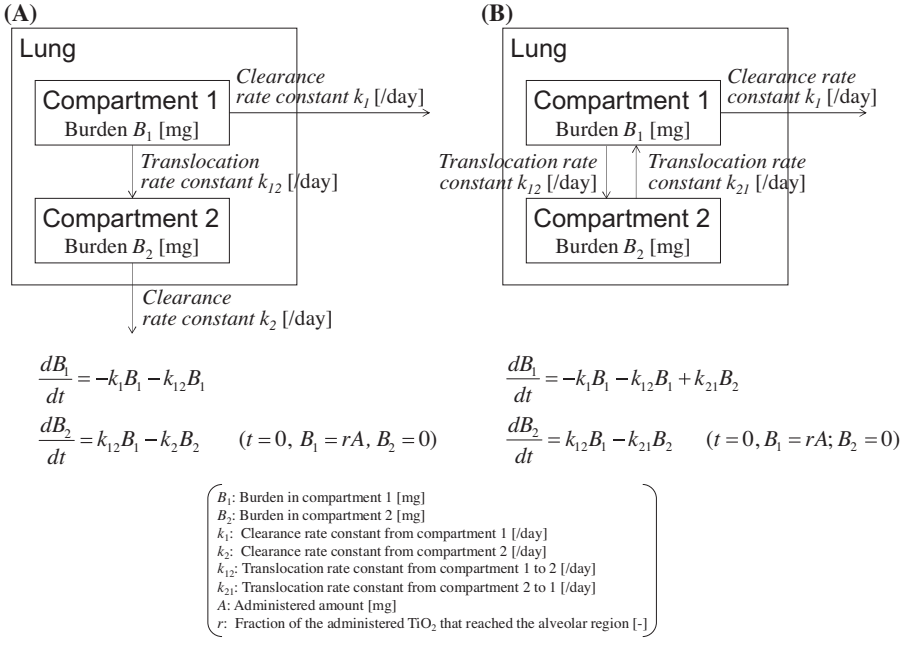

Fig. 2. (A) 2-compartment model A in which TiO_2 nanoparticles are cleared from compartments 1 and 2 and (B) 2-compartment model B in which TiO_2 nanoparticles are cleared from compartment 1 and translocate from compartments 2 to 1. The models A and B are expressed in a first-order decay equation with rate constants k_1,k_{12}, and k_2, and with rate constants k_1, k_{12}, and k_{21}, respectively.

in lung compartment 1 (mg); B_2 was the TiO_2 burden in lung compartment 2 (mg); A was the amount of TiO_2 administered (mg); r was the fraction of the administered TiO_2 that reached the alveolar region; and k_1, k_{12}, and k_2 were the rate constants for clearance from compartment 1 (/day), translocation from compartment 1 to 2 (/day), and clearance from compartment 2 (/day), respectively.

$$\frac{dB_1}{dt} = -k_1 B_1 - k_{12} B_1 \quad (2)$$

$$\frac{dB_2}{dt} = k_{12}\, B_1 - k_2 B_2 \quad (t = 0, B_1 = rA; B_2 = 0) \quad (3)$$

The 2-compartment model B can be represented by a clearance from compartment 1 and reciprocal translocation between compartment 1 and 2 as shown in Eqs. (4) and (5), where k_{21} was the rate constant for translocation from compartment 1 to 2 (/day).

$$\frac{dB_1}{dt} = -k_1 B_1 - k_{12} B_1 + k_{21} B_2 \quad (4)$$

$$\frac{dB_2}{dt} = k_{12}\, B_1 - k_{21}\, B_2 \quad (t = 0, B_1 = rA; B_2 = 0) \quad (5)$$

The clearance/translocation rate constants, k, k_1, k_{12}, k_2, and, k_{21} and the fraction of the administered TiO_2 that reached the alveolar region, r, of each model were estimated by fitting the decay curve to the total TiO_2 burden measured in the lungs including BALF.

Curve fitting was conducted using a least squares approach, in which the following sum of square difference in the logarithmic converted lung burden between the measured lung burden (B_{measured}), and the estimated lung burden ($B_1 + B_2$) was minimized (Eq. (6)), using the Solver tool in Excel 2010.

$$\text{Sum of square difference} = \sum \left(\text{Ln}B_{\text{measured}} - \text{Ln}(B_1 + B_2)\right)^2 \quad (6)$$

2.5. TiO_2 translocation rate coefficients to thoracic lymph nodes

The rate constants for translocation of TiO_2 from lung to thoracic lymph nodes were estimated under the following two assumptions, applied to the 2-compartment models A and B. One assumption was that TiO_2 translocated from compartment 1 to the thoracic lymph nodes (Eq. (7)) and the other assumption was that TiO_2 translocated from compartment 2 to the thoracic lymph nodes (Eq. (8)).

$$\frac{dB_{\text{Lym}}}{dt} = k_{\text{Lung}\rightarrow\text{Lym}} B_1 \quad (t = 0, B_{\text{Lym}} = 0) \quad (7)$$

$$\frac{dB_{\text{Lym}}}{dt} = k_{\text{Lung}\rightarrow\text{Lym}} B_2 \quad (t = 0, B_{\text{Lym}} = 0) \quad (8)$$

Where, B_{Lym} was the total TiO_2 burden in the right and left posterior mediastinal lymph nodes, and the parathymic lymph nodes (μg); B_1 was the TiO_2 lung burden in compartment 1 (μg); B_2 was the TiO_2 lung burden in compartment 2 (μg); and $k_{\text{Lung}\rightarrow\text{Lym}}$ was the translocation rate constant from lung to thoracic lymph nodes (/day).

The least squares method was used for the estimation (Eq. (9)).

$$\text{Sum of square difference} = \sum \left(\text{Ln}B_{\text{Lym}_{\text{measured}}} - \text{Ln}B_{\text{Lym}_{\text{estimated}}}\right)^2 \quad (9)$$

Where $B_{\text{Lym\_measured}}$ was the measured thoracic lymph node TiO_2 burden and $B_{\text{Lym\_estimated}}$ was the estimated thoracic lymph node TiO_2 burden.

2.6. Statistical analysis

The differences in tissue Ti or TiO_2 concentrations between the study groups were statistically analyzed by Student's t test or one-way ANOVA (Welch's test) after F-testing using SPSS 20.0.

3. Results

3.1. TiO_2 nanoparticle characteristics

The Z-average particle sizes were 143–148 nm in the administered suspensions, with ζ potentials of −44 mV. Fig. 3 shows the TiO_2 nanoparticle size distribution and a scanning electron micrograph of the nanoparticle in the stock suspension. The specific surface area of TiO_2 nanoparticles in the administered suspension was 59 m^2/g, which was very similar to that of the primary particles (50 ± 15 m^2/g, catalog value).

3.2. Ti content in the dosing suspensions, drinking water, and rat feed

The TiO_2 concentrations in the diluted suspensions, determined by ICP-AES, were >95% of the concentration estimated by weight measurement and accounting for the dilution factor. Thus, the concentration of the stock solution was confirmed. The concentrations of Ti in drinking water and feed, determined by ICP-SFMS, were <0.10 ng/mL and 2700 ng/g, respectively. This corresponded to TiO_2-equivalent concentrations of <0.17 ng/mL and 4500 ng/g, respectively.

3.3. Organ TiO_2 burdens

TiO_2 burdens in lung after BALF sampling, BALF, and trachea between 1 day and 26 weeks after administration of TiO_2

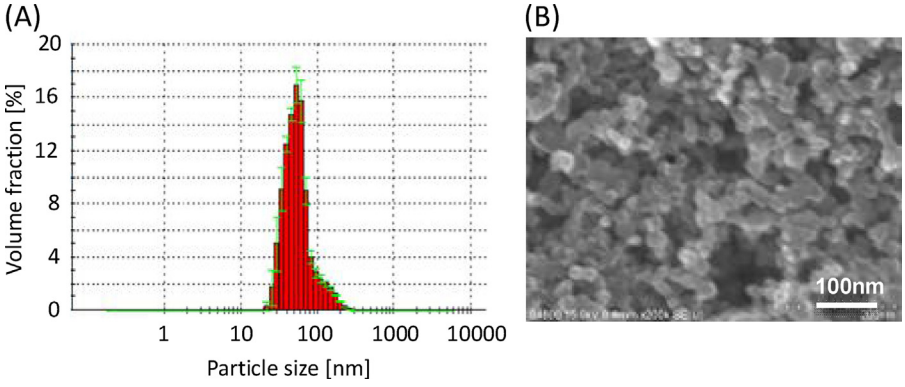

Fig. 3. (A) Size distribution and (B) scanning electron micrograph of the TiO_2 nanoparticle suspension used for intratracheal administration.

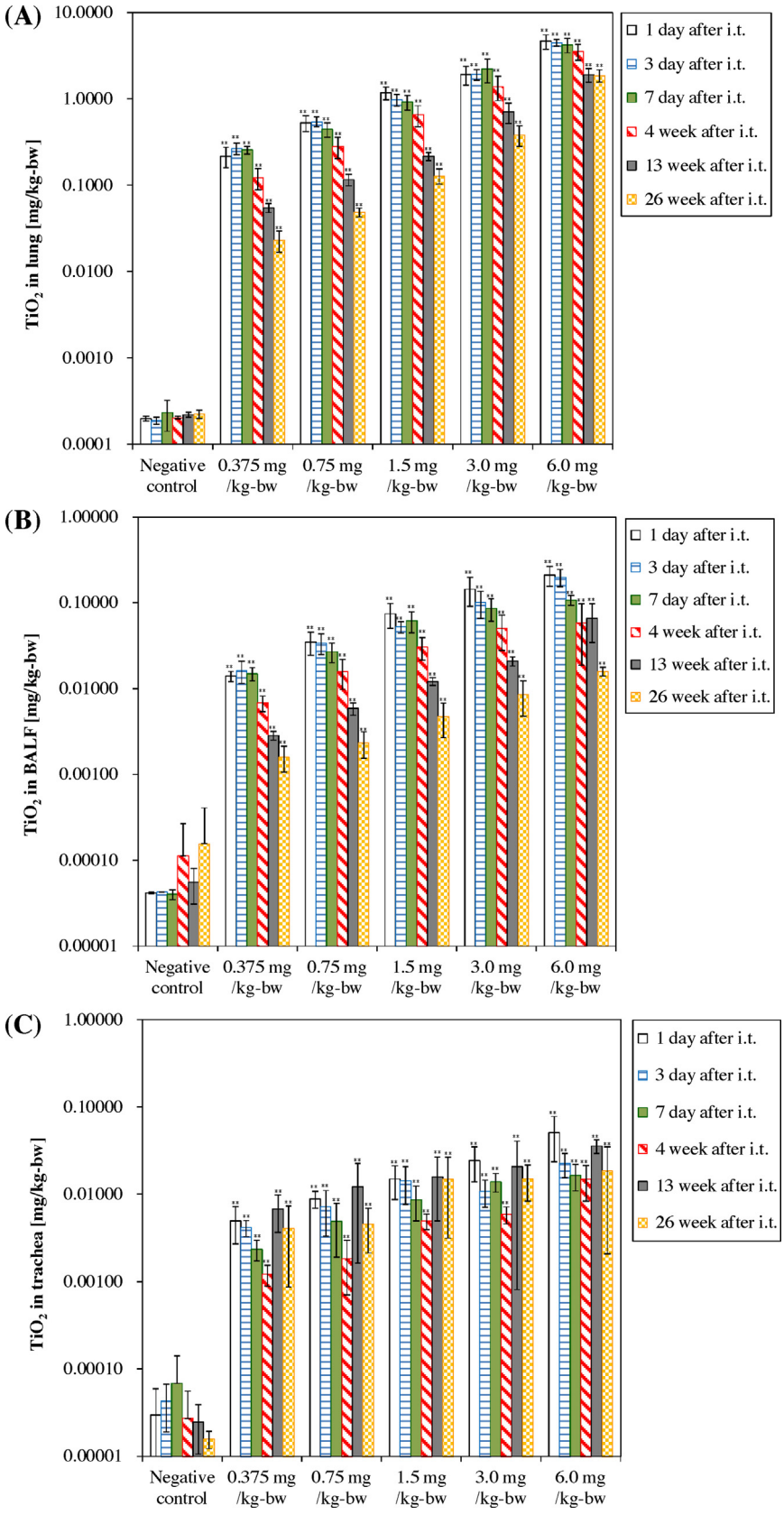

Fig. 4. TiO_2 burden per initial body weight in (A) lung, (B) BALF, and (C) trachea after intratracheal administration of nanoparticles. The columns and error bars indicate the mean and standard deviation, respectively. Asterisks indicate statistically significant differences, compared with the control group (** $P < 0.01$, * $P < 0.05$). Samples with TiO_2 levels below the quantification limit were assigned values corresponding to half the quantification limit.

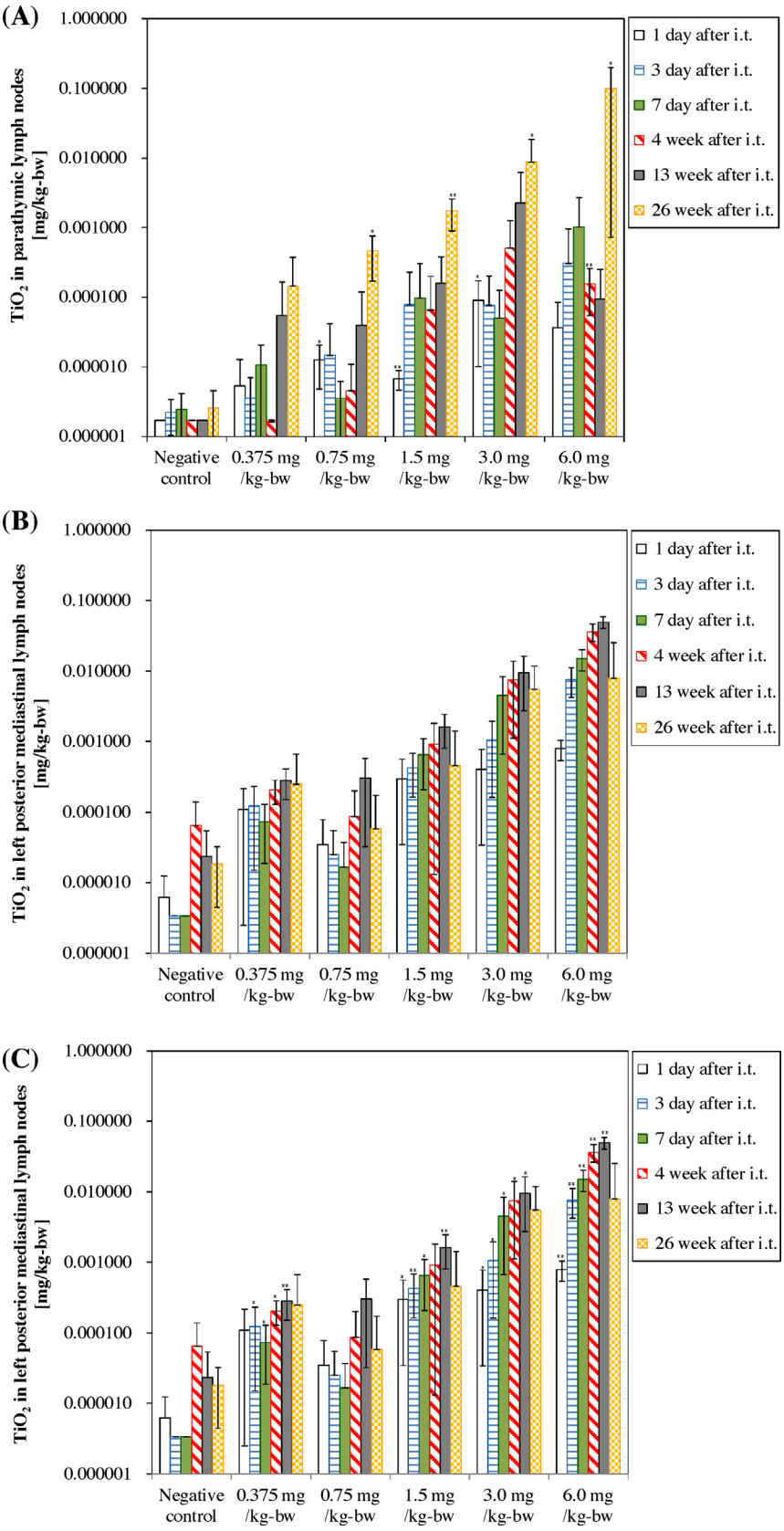

Fig. 5. TiO_2 burden per initial body weight in (A) right posterior mediastinal lymph nodes, (B) left posterior mediastinal lymph nodes, and (C) parathymic lymph nodes, following intratracheal nanoparticle administration. The columns and error bars indicate the mean and standard deviation, respectively. Asterisks indicate statistically significant differences, compared with the control group (** $P < 0.01$, * $P < 0.05$). Samples with TiO_2 levels below the quantification limit were assigned values corresponding to half the quantification limit.

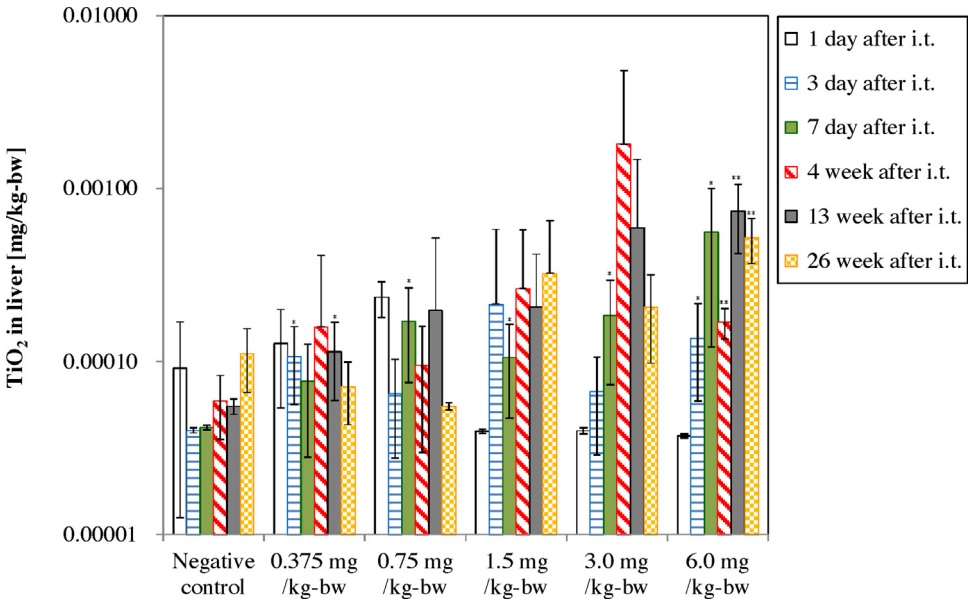

Fig. 6. TiO_2 burden per initial body weight in liver. The columns and error bars indicate the mean and standard deviation, respectively. Asterisks indicate statistically significant differences, compared with the control group (** $P < 0.01$, * $P < 0.05$). Samples with TiO_2 levels below the quantification limit were assigned values corresponding to half the quantification limit.

nanoparticles were significantly higher ($P < 0.01$) than those of the control group (Fig. 4). The rat TiO_2 burden depended on the dose administered. TiO_2 burdens in lung after BALF sampling and BALF decreased over time. One day after administration, 58% ± 16%, 70% ± 15%, 78% ± 13%, 64% ± 15%, and 77% ± 15% of the TiO_2 administered was present in the lungs after BALF sampling of rats dosed with 0.375, 0.75, 1.5, 3.0, and 6.0 mg/kg, respectively, while 6.1% ± 1.7%, 6.5% ± 0.75%, 8.6% ± 1.7%, 13% ± 3.4%, and 31% ± 4.9% of administered TiO_2 was present in the lungs after BALF sampling 26 weeks after administration of 0.375, 0.75, 1.5, 3.0, and 6.0 mg/kg, respectively. Much less TiO_2 was detected in BALF or trachea following intratracheal administration of TiO_2 nanoparticles. In BALF, 3.7% ± 0.49%, 4.6% ± 1.4%, 4.9% ± 1.6%, 4.8% ± 1.8%, and 3.5% ± 0.90% of the TiO_2 administered was present 1 day after administration of 0.375, 0.75, 1.5, 3.0, and 6.0 mg/kg, respectively, as compared with 0.43% ± 0.14%, 0.31% ± 0.11%, 0.31% ± 0.14%, 0.28% ± 0.13%, and 0.26% ± 0.031% detected in BALF 26 weeks after administration. In trachea, 1.3% ± 0.60%, 1.2% ± 0.26%, 1.0% ± 0.41%, 0.81% ± 0.35%, and 0.84% ± 0.45% of 0.375, 0.75, 1.5, 3.0, and 6.0 mg/kg TiO_2, respectively, was present 1 day after administration, as compared to 1.1% ± 0.85%, 0.60% ± 0.32%, 0.98% ± 0.78%, 0.50% ± 0.22%, and 0.31% ± 0.27% in the trachea at 26 weeks after administration.

TiO_2 burdens in the thoracic lymph nodes are shown in Fig. 5. The TiO_2 burdens in most of the thoracic lymph nodes were significantly higher in the groups dosed with TiO_2 nanoparticles, compared with the control group, and increased over time. The total thoracic lymph node burden (right and left posterior mediastinal lymph nodes, and parathymic lymph nodes) ranged from 0.0089–0.040% of the dose administered 1 day after intratracheal administration. The TiO_2 burden in thoracic lymph nodes showed dose-dependency 26 weeks after administration,

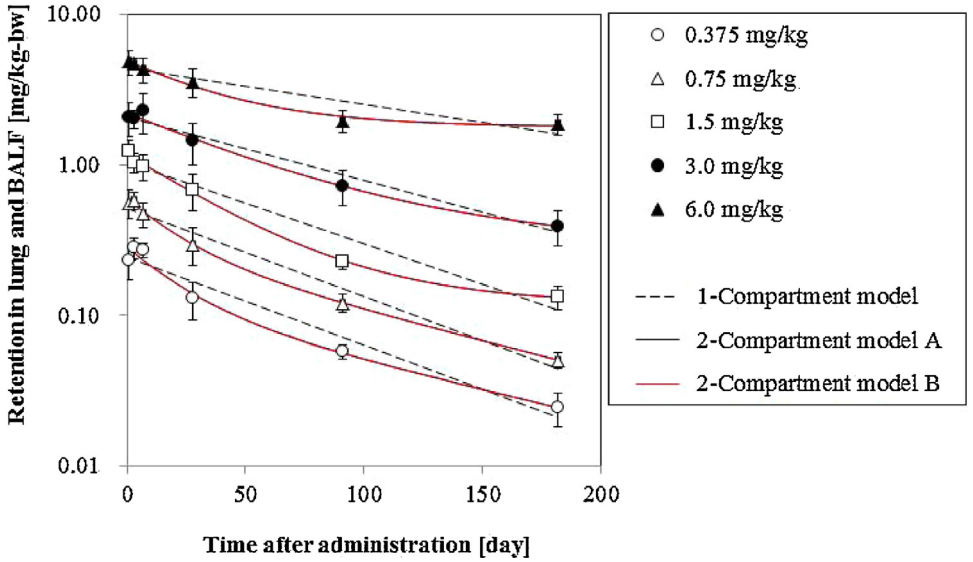

Fig. 7. Model fitting to the experimental data relating to lung and BALF TiO_2 burdens per initial body weight. The solid line shows the 2-compartment model fitting and the broken line shows the 1-compartment model fitting.

Table 1
Pulmonary clearance rate constants, translocation rate constants, and initial fraction of the administered TiO_2 that reached the alveolar region estimated using the lung and BALF burden data (A) using 1-compartment model, (B) using 2-compartment model A, and (C) using 2-compartment model B.

(A) Dose (mg/kg)	k (/day)	Initial fraction of the administered TiO_2 that reached the alveolar region (%)	Sum of square difference
0.375	0.013	65	0.21
0.75	0.013	69	0.13
1.5	0.012	69	0.23
3.0	0.010	69	0.075
6.0	0.0055	73	0.13

(B) Dose (mg/kg)	k_1 (/day)	k_{12} (/day)	k_2 (/day)	Initial fraction of the administered TiO_2 that reached the alveolar region (%)	Sum of square difference
0.375	0.030	0.015	0.0086	76	0.069
0.75	0.030	0.018	0.0093	80	0.0057
1.5	0.022	0.0025	0.0000	79	0.015
3.0	0.014	0.0027	0.00082	74	0.025
6.0	0.016	0.0092	0.0000	82	0.011

(C) Dose (mg/kg)	k_1 (/day)	k_{12} (/day)	k_{21} (/day)	Initial fraction of the administered TiO_2 that reached the alveolar region (%)	Sum of square difference
0.375	0.030	0.011	0.013	76	0.069
0.75	0.030	0.012	0.015	80	0.0057
1.5	0.022	0.0025	0.0000	79	0.015
3.0	0.014	0.0025	0.00098	74	0.025
6.0	0.016	0.0092	0.0000	82	0.011

with 0.18% ± 0.13%, 0.10% ± 0.055%, 0.37% ± 0.22%, 1.3% ± 0.45%, and 3.4% ± 1.2% for the doses of 0.375, 0.75, 1.5, 3.0, and 6.0 mg/kg, respectively.

TiO_2 burdens in liver are shown in Fig. 6. The liver TiO_2 burden was significantly elevated above control levels only in the animals administered 6.0 mg/kg at 3 days to 26 weeks after the administration ($P < 0.01$). In these groups, the liver TiO_2 burden was 0.0023% ± 0.0013%, 0.0094% ± 0.0073%, 0.0028% ± 0.00056%, 0.012% ± 0.0053%, and 0.0087% ± 0.0025% of the dose administered at 3 days, 7 days, 4 weeks, 13 weeks, and 26 weeks after administration, respectively. No significant differences were observed in kidney and spleen TiO_2 levels in animals treated with the higher dose of nanoparticles and in control animals.

3.4. TiO_2 clearance analysis using compartment models

The 2-compartment models were found to provide a better description of the pulmonary TiO_2 burden decay curves than the 1-compartment model, as shown in Fig. 7. The sum of square difference was 0.006–0.07 for the 2-compartment models A and B and 0.07–0.2 for the 1-compartment model. Since fitting results did not differ significantly between the 2-compartment models A and B, we have mainly shown the results of 2-compartment model A below. The estimated fraction of the administered TiO_2 that reached the alveolar region and clearance/translocation rate constants based on the 1- compartment model and 2-compartment model A are shown in Table 1. The clearance rate

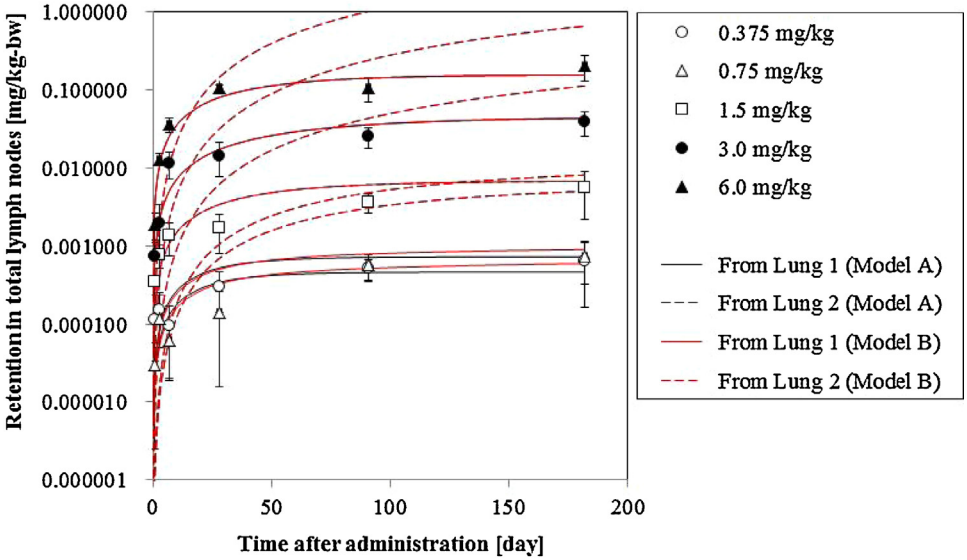

Fig. 8. Model fitting to the experimental data relating to total thoracic lymph nodes TiO_2 burden per initial body weight. The solid line shows the fitting curve for translocation from compartment 1 to thoracic lymph nodes and the broken line shows the fitting curve for translocation from compartment 2 to thoracic lymph nodes.

Table 2
Translocation rate constant from lung to thoracic lymph nodes, $k_{Lung \rightarrow Lym}$. (A) Assuming translocation from compartment 1 to thoracic lymph nodes and (B) assuming translocation from compartment 2 to thoracic lymph nodes.

(A) Dose (mg/kg)	$k_{Lung \rightarrow Lym}$ (/day)	Sum of square difference
0.375	0.00012	2.8
0.75	0.000037	2.1
1.5	0.00014	1.6
3.0	0.00035	0.88
6.0	0.00081	0.92

(B) Dose (mg/kg)	$k_{Lung \rightarrow Lym}$ (/day)	Sum of square difference
0.375	0.0010	33
0.75	0.00028	23
1.5	0.0066	35
3.0	0.016	26
6.0	0.010	21

constants estimated by the 1-compartment model were stable (0.012–0.013/day) between the doses of 0.375 and 1.5 mg/kg, and decreased to 0.0097 and 0.0055/day at doses of 3.0 and 6.0 mg/kg, respectively. In the 2-compartment model, the clearance rate constants from compartment 1, k_1, estimated using model A decreased from 0.030 (0.375 and 0.75 mg/kg) to 0.014 and 0.016/day (3.0 and 6.0 mg/kg) with increasing TiO_2 dose. The translocation rate constants from compartment 1 to 2, k_{12}, estimated for doses of 0.375 and 0.75 mg/kg, 0.015 and 0.018/day, were higher than those for doses of 1.5–6.0 mg/kg, 0.0025–0.0092/day. The clearance rate constants from compartment 2, k_2, were also higher for doses of 0.375 and 0.75 mg/kg, 0.0086 and 0.0093/day, than those for doses of 1.5–6.0 mg/kg, 0–0.00082/day.

3.5. TiO_2 translocation rate coefficients to thoracic lymph nodes

Measured and estimated TiO_2 burden in thoracic lymph nodes are shown in Fig. 8. The sum of square differences indicated that the estimated thoracic lymph node burdens were a much better fit to the measured burdens when TiO_2 translocation from compartment 1 to the thoracic lymph nodes was assumed, rather than those where TiO_2 translocation from compartment 2 to the thoracic lymph nodes was assumed (Table 2). The sum of square difference was 0.9–3 for the former assumption, and 20–40 for the latter assumption. The translocation rate coefficients from the lungs to the thoracic lymph nodes ($k_{Lung \rightarrow Lym}$) estimated under the former assumption, increased depending on the TiO_2 dose, with $k_{Lung \rightarrow Lym}$ of 0.000037–0.00012/day for doses of 0.375–1.5 mg/kg to 0.00035 and 0.00081/day for doses of 3.0 and 6.0 mg/kg, respectively.

4. Discussion

In the results of 2-compartment model fitting, the fraction of the administered TiO_2, that reached to alveolar region which does not include the bronchi and bronchiole, was estimated to be 74–82%, and this was not dose-dependent. Approximately 20% of the administered dose was considered not to have reached to the alveolar region, but to be trapped in the bronchi and bronchioles, from where it was subsequently excreted by the bronchial mucociliary escalator.

In this study, a certain fraction of the TiO_2 nanoparticles (0.4–1.5%) was stably detected in the trachea at 1 day to 26 weeks after intratracheal administration; this fraction was not dose-dependent. Particles deposited on the bronchi and bronchioles can be cleared by the bronchial mucociliary escalator within 5 min because the bronchial length (throat to terminal bronchiole) in rats is approximately 53 mm (Yeh et al., 1979) and ciliary motion rates are 7.5–13.6 mm/min (Lightowler and Williams, 1969). It is probably incorrect to assume that all of the TiO_2 detected in the trachea in the present study (0.4–1.5% of the administration dose) was in the process of being cleared from the alveoli by the bronchial mucociliary escalator, as this would lead to the unrealistic conclusion that all of the administered TiO_2 could be cleared via this route within 1 day. Some TiO_2 particles might be retained in the trachea until at least 26 weeks after the administration.

In the present study, lavagable fractions of TiO_2 nanoparticle in lung (BALF/(lung + BALF)) were 4.4–7.0% 1 day after administration and 0.84–6.5% 26 weeks after administration. Although the lavagable fraction was constant at lower doses (6.1% and 6.2% at 1 day to 6.5% and 4.6% at 26 weeks after administration for 0.375 and 0.75 mg/kg), it decreased at higher doses (4.4–7.0% at 1 day to 0.84–3.5% at 26 weeks after administration for 1.5–6.0 mg/kg). At higher doses, this low fraction could be associated with delayed clearance from lung. Previous studies indicated that the lavagable fraction of ultrafine TiO_2 particles in lung corresponded to 69%, which was calculated using the tissue fraction (15.4%) and the equation (Tissue fraction = $1 - 1.23 \times$ lavaged fraction), 1 day after intratracheal administration of approximately 2.3 mg/kg (0.5 mg/rat) (Oberdörster et al., 1992) and 19% 7 days after intratracheal administration of approximately 2 mg/kg (0.52 mg/rat) (Sager et al., 2008). In the present study, 6.0% and 7.0% of the administered TiO_2 nanoparticles were lavaged 1 day after administration of 1.5 and 3.0 mg/kg, respectively, and 6.3% and 3.8% 7 days after administration of 1.5 and 3.0 mg/kg. Therefore, comparing similar doses and observation timings, the fractions in the present study were smaller than those reported previously. In these three studies, the animals were of the same strain and sex (Fisher F344 rat; male) and their body weight were similar (220 g in Oberdörster et al. (1992), 200–300 g in Sager et al. (2008); and 215–273 g in our study). The primary sizes of the TiO_2 nanoparticles were also similar among the three studies: ~20 nm in Oberdörster et al. (1992) and 21 nm in Sager et al. (2008) and in our study. However, BALF was sampled using 2×7 mL washes with saline in the present study, compared to 10×5 mL washes (Oberdörster et al., 1992) or 2×6 mL washes followed by several 8 mL washes, up to a total of 80 mL (Sager et al., 2008). This was consistent with our observation of fewer macrophages and neutrophils in BALF, compared to those reported in previous studies (Table S1) (Oberdörster et al., 1992; Sager et al., 2008). Therefore, the smaller fraction in the present study could be due to the milder BALF sampling.

The lavagable fraction in the present study could be either the particles internalized in the lavagable alveolar macrophages and/or the free particles in the airspaces. Oberdörster et al. (1992) considered that 1.23 times the lavagable fraction is retained in the alveolar space and the rest is located in the tissue. Sager et al. (2008) considered the lavagable fraction as the particles internalized by lavagable alveolar macrophages or presenting as free particles in the airspaces. Since BALF sampling was milder in our study than in the previous studies, the number of particles in lavagable macrophages and/or free particles in the air space might be larger than the lavagable fraction obtained in the present study.

In previous studies, after inhalation exposure to TiO_2 nanoparticles, TiO_2 was only detected in the lungs and lung-associated lymph nodes, and was below the detection limit of <500 ng/organ in other organs (Bermudez et al., 2004; Ma-Hock et al., 2009; van Ravenzwaay et al., 2009). The present study used highly sensitive analytical methods and the detection limit improved to permit detection of considerably lower levels of tissue TiO_2 (detection limits: 30 ng/organ in lung; 1.0 ng/organ in trachea; 0.5 ng/organ in lymph nodes; 14 ng/organ in liver), enabling determination of TiO_2

distribution for organs where TiO_2 content could not be determined in previous studies. This identified a liver TiO_2 burden of 34–180 ng/organ (0.0023–0.012%) from 3 days to 26 weeks after administration of 6.0 mg/kg, which was significantly higher than the level detected in the control group (9.8–27 ng/organ), and which would have been below the limit of detection (500 ng/organ) in the previous studies. This suggested that some pulmonary TiO_2 nanoparticles could translocate to the liver via the blood. Although TiO_2 nanoparticles might translocate from lung to liver at 0.375–3.0 mg/kg, we could not observe significant results because of the variance in the negative control. Since >90% of intravenously injected TiO_2 (P25) nanoparticles translocated to the liver within 1 day and were rarely cleared from it, even after 30 days (Shinohara et al., 2014), the burden detected in liver could be considered to represent translocation from the lung to blood and it is possible that translocation from the lung to other organs (apart from the liver) was negligible. In the present study, spleen and kidney TiO_2 levels did not differ between the groups administered TiO_2 nanoparticles and the control group.

Delayed pulmonary clearance of TiO_2 nanoparticles was found at higher doses, a phenomenon that is termed overload. Using the 1-compartment model, the clearance rate constant, k, did not vary at doses of between 0.375 and 1.5 mg/kg, and decreased at 3.0 and 6.0 mg/kg. This result was consistent with the findings of a 12-month observation study after intratracheal instillation (Oyabu et al., 2013), where pulmonary clearance of intratracheally-administered TiO_2 nanoparticles was observed to be delayed at high doses of 3.3 mg/kg and 10 mg/kg, compared with those observed at low doses of 0.33 mg/kg and 0.66 mg/kg, using the 1-compartment model.

The present study found that 3.4% ± 1.2% of the 6.0 mg/kg TiO_2 nanoparticle dose had translocated to thoracic lymph nodes by 26 weeks after administration. Translocation to thoracic lymph nodes similarly increased over time after inhalation exposure in previous studies (Bermudez et al., 2004). In the present study, translocation to thoracic lymph nodes was estimated to occur from compartment 1 according to the comparison of curve fitting between 2 assumptions. The dose-dependent increase observed in $k_{Lung \rightarrow Lym}$ in the present study suggested that the translocation to thoracic lymph nodes was enhanced at higher nanoparticle doses unlike pulmonary clearance. Therefore, pulmonary overload was considered not to be associated with the thoracic lymph node clearance route. Since the translocation rate constants ($k_{Lung \rightarrow Lym}$) were independently estimated for given burdens in compartments 1 and 2 (B_1 and B_2) estimated with the 2-compartment model, the translocation rate constants, $k_{Lung \rightarrow Lym}$, could be considered to be the part of the clearance rate constants from compartment 1, k_1. Although the ratio of $k_{Lung \rightarrow Lym}$ to k_1 showed a dose-dependent increase (0.4% at 0.375 mg/kg to 5% at 6.0 mg/kg), most clearance from lung could occur via other routes, such as the bronchial mucociliary escalator. In the previous compartmental models for pulmonary clearance, compartments 1 and 2 were considered to be the alveolar surface and the interstitium, respectively, and the clearance pathways from compartment 1 and 2 were considered to be the bronchial mucociliary escalator via the bronchi, and translocation to lung-associated lymph nodes via the interstitium, respectively (Stöber, 1999; Kuempel et al., 2001). In the present study, however, it was suggested that clearances both by the bronchial mucociliary escalator via the bronchi after macrophage phagocytosis and translocation to the thoracic lymph nodes should be described as clearance from compartment 1. Therefore, it is better to consider compartment 2 as a lung compartment where particle accumulate, rather than as an intermediate compartment for slow particle clearance. Compartment 2 might correspond to macrophages which have phagocytosed TiO_2 nanoparticles and have subsequently been sequestered within the interstitium.

Measured pulmonary burden can be well modeled effectively using the classical 2-compartment model in the present study. The advantage of the classical model in the present study over the previous physiologically based models is that it eliminates the arbitrariness and uncertainty in deciding the clearance mechanism and compartment meanings because the clearance mechanism and compartment meanings do not have to be predicted in advance. On the other hand, the disadvantage of the current model is that the meaning of the compartments is assumed only on the basis of circumstantial evidence. In addition, fitting of the results could be unclear if there is only a small amount of data.

In the results of 2-compartment model fitting, the k_1 (0.014–0.030/day, equivalent half-life: 23–48 days) was higher than the k_{12} (0.0025–0.018/day, equivalent half-life: 39–280 days), and the k_2 (0–0.0093/day, equivalent half-life: 75–>840 days) (Table 1B). The rate constants for clearance from compartment 1, k_1, and translocation from compartments 1 to 2, k_{12}, were lower at doses of 1.5–6.0 mg/kg than at doses of 0.375 and 0.75 mg/kg. The rate constants for clearance from compartment 2, k_2, (or transfer rate constants from compartment 2 to 1, k_{21}) were much lower at doses of 1.5–6.0 mg/kg than at doses of 0.375 and 0.75 mg/kg. One of possible mechanism that could explain these dose-dependencies would be follows. Both clearance via the bronchial mucociliary escalator, and the sequestration of macrophages that have ingested TiO_2, showed dose-dependent reductions. In addition, small amounts of TiO_2 nanoparticle in the sequestrum macrophages could be cleared, or the macrophages could become non-sequestrum, at lower nanoparticle doses. However, at higher TiO_2 nanoparticle doses, almost no TiO_2 nanoparticles could be cleared from the sequestrum macrophages and they could not be cleared from the sequestrum macrophages or they could not become non-sequestrum.

5. Conclusion

In the present study, the tissue distribution and clearance of TiO_2 nanoparticles (P25) were determined after intratracheal administration to rats, using highly sensitive analytical methods. By 26 weeks after administration, the lung TiO_2 burden including BALF had decreased to 6.6–8.9% of the 0.375–1.5 mg/kg doses and to 13% and 31% of the 3.0 and 6.0 mg/kg doses. At higher doses, pulmonary clearance was inhibited. The pulmonary clearance rate constants k_1, k_{12}, and k_2, estimated to be 0.014–0.030, 0.0025–0.018, and 0.0000–0.0093/day using a 2-compartment model, decreased in a dose-dependent manner. The translocation rate constants from lung to thoracic lymph nodes, $k_{Lung \rightarrow Lym}$, estimated to be 0.000037–0.00081/day, were much lower than these pulmonary clearance rate constants and increased in a dose-dependent manner.

Conflict of interest

This work is part of the research program “Development of innovative methodology for safety assessment of industrial nanomaterials” supported by the Ministry of Economy, Trade and Industry (METI) of Japan.

Transparency document

The Transparency document associated with this article can be found in the online version.

Appendix A Supplementary data

Supplementary data associated with this article can be found, in the online version, at http://dx.doi.org/10.1016/j.tox.2014.08.003.

References

Bermudez, E., Mangum, J.B., Wong, B.A., Asgharian, B., Hext, P.M., Warheit, D.B., Everitt, J.I., 2004. Pulmonary responses of mice rats, and hamsters to subchronic inhalation of ultrafine titanium dioxide particles. Toxicol. Sci. 77, 347–357.

De Jong, W.H., Hagens, W.I., Krystek, P., Burger, M.C., Sips, A.J.A.M., Geertsma, R.E., 2008. Particle size-dependent organ distribution of gold nanoparticles after intravenous administration. Biomaterials 29, 1912–1919.

Donaldson, K., Stone, V., Clouter, A., Renwick, L., MacNee, W., 2001. Ultrafine particles. Occup. Environ. Med. 58, 211–216.

Donaldson, K., Stone, V., Tran, C.L., Kreyling, W., Borm, P.J., 2004. Nanotoxicology. Occup. Environ. Med. 61, 727–728.

Fuji Chimera Research Institute, Inc. , 2009. Metallic Oxide 10. Ultrafine Particle Titanium Dioxide, Metallic Oxide 12. Titanium Dioxide for Photocatalyst, III. Market Compilation by Commodity Item, Current State and Future Outlook of the Ultrafine Particle Market in 2009. (Japanese).

Kuempel, E.D., O'Flaherty, E.J., Stayner, L.T., Smith, R.J., Green, F.H.Y., Vallyathan, V., 2001. A biomathematical model of particle clearance and retention in the lungs of coal miners - I Model development. Regul. Toxicol. Pharmacol 34, 69–87.

Lightowler, N.M., Williams, J.R., 1969. Tracheal mucus flow rates in experimental bronchitis in rats. Br. J. Exp. Pathol. 50, 139–149.

Ma-Hock, L., Burkhardt, S., Strauss, V., Gamer, A., Wiench, K., van Ravenzwaay, B., Landsiedel, R., 2009. Development of a short-term inhalation test in the rat using nano-titanium dioxide as a model substance. Inhal. Toxicol 21, 102–118.

Morrow, P.E., 1992. Dust overloading of the lungs - update and appraisal. Toxicol. Appl. Pharmacol 113, 1–12.

Oberdörster, G., Ferin, J., Gelein, R., Soderholm, S.C., Finkelstein, J., 1992. Role of the alveolar macrophage in lung injury - studies with ultrafine particles. Environ. Health Perspect 97, 193–199.

Oberdörster, G., Oberdörster, E., Oberdörster, J., 2005. Nanotoxicology: an emerging discipline evolving from studies of ultrafine particles. Environ. Health Perspect 113, 823–839.

Oyabu, T., Morimoto, Y., Hirohashi, M., Horie, M., Kambara, T., Lee, B.W., Hashiba, M., Mizuguchi, Y., Myojo, T., Kuroda, E., 2013. Dose-dependent pulmonary response of well-dispersed titanium dioxide nanoparticles following intratracheal instillation. J. Nanopart. Res 15, 1600.

Rehn, B., Seiler, F., Rehn, S., Bruch, J., Maier, M., 2003. Investigation on the inflammatory and genotoxic lung effects of two types of titanium dioxide: untreated and surface treated. Toxicol. Appl. Pharmacol 189, 84–95.

Sager, T.M., Kommineni, C., Castranova, V., 2008. Pulmonary response to intratracheal instillation of ultrafine versus fine titanium dioxide: role of particle surface area. Part. Fibre Toxicol. 5, 17.

Shinohara, N., Nakazato, T., Tamura, M., Endoh, S., Fukui, H., Morimoto, Y., Myojo, T., Shimada, M., Yamamoto, K., Tao, H., Yoshida, Y., Nakanishi, J., 2010. Clearance kinetics of fullerene C_{60} nanoparticles from rat lungs after intratracheal C_{60} instillation and inhalation C_{60} exposure. Toxicol. Sci 118, 564–573.

Shinohara, N., Danno, N., Ichinose, T., Sasaki, T., Fukui, H., Honda, K., Gamo, M., 2014. Tissue distribution and clearance of intravenously administered titanium dioxide (TiO_2) nanoparticles. Nanotoxicology 8, 132–141.

Stöber, W., 1999. POCK model simulations of pulmonary quartz dust retention data in extended inhalation exposures of rats. Inhal Toxicol. 11, 269–292.

van Ravenzwaay, B., Landsiedel, R., Fabian, E., Burkhardt, S., Strauss, V., Ma-Hock, L., 2009. Comparing fate and effects of three particles of different surface properties Nano-TiO_2, pigmentary TiO_2 and quartz. Toxicol. Lett. 186, 152–159.

Warheit, D.B., Webb, T.R., Reed, K.L., Frerichs, S., Sayes, C.M., 2007. Pulmonary toxicity study in rats with three forms of ultrafine-TiO_2 particles: Differential responses to surface properties. Toxicology 230, 90–104.

Yeh, H.C., Schum, G.M., Duggan, M.T., 1979. Anatomic models of the tracheobronchial and pulmonary regions of the rat. Anat. Rec. 195 483, 492.